

## CAV2009 – Paper No. 103

### Cavitation as a Microfluidic Tool

**Claus-Dieter Ohl**

Division of Physics and Applied Physics  
School of Physical and Mathematical Sciences  
Nanyang Technological University  
Singapore

**Pedro Antonio Quinto-Su**

Division of Physics and Applied Physics  
School of Physical and Mathematical Sciences  
Nanyang Technological University  
Singapore

**Rory Dijkink**

Physics of Fluids  
Faculty of Sciences  
University of Twente, Enschede,  
The Netherlands

**Roberto Gonzalez**

Division of Physics and Applied Physics  
School of Physical and Mathematical Sciences  
Nanyang Technological University  
Singapore

**Firdaus Prabowo**

Division of Physics and Applied Physics  
School of Physical and Mathematical Sciences  
Nanyang Technological University  
Singapore

**Xiaohu Huang**

Division of Physics and Applied Physics  
School of Physical and Mathematical Sciences  
Nanyang Technological University  
Singapore

**Tom Wu**

Division of Physics and Applied Physics  
School of Physical and Mathematical Sciences  
Nanyang Technological University  
Singapore

**Vasan Venugopalan**

Department of Chemical Engineering & Materials Science and  
Laser Microbeam and Medical Program, Beckman Laser Institute,  
University of California, Irvine, CA,  
U.S.

#### ABSTRACT

Cavitation in confined geometries in particular in narrow gaps prevalent in microfluidic geometries allows for novel applications. Here we will give an overview of successful demonstrations of cavitation as a microfluidic tool.

Cavitation can pump and mix liquids very rapidly, move objects such as cells, rupture plasma membranes, probe elastic properties in micro-rheology, study coalescence, and even create arbitrary superpositions of shock waves. In all areas, bubbles are created with a focused laser which allows precise temporal and spatial control. With the usage of digital holography arbitrary configurations of bubbles can be created such as bubble clusters, squarish, toroidal, or even linear cavitation bubbles.

Interestingly, even in very narrow gaps of a few tens of microns most of the bubble dynamics can be described with potential flow. This presentation will summarize published work and show current research under progress.

#### INTRODUCTION

Cavitation in narrow gaps has received considerable interest because of its importance in the research of damage in bearings, e.g. [1]. In 2006 Chen *et al.* [2] demonstrated cavitation induced with a pulsed laser in a narrow fluid gap of 10 $\mu$ m. Due to its high reproducibility the bubble dynamics could be studied with stroboscopic recordings. Zwaan *et al.* [3] applied this technique to a microfluidic system made of PDMS (Polydimethylsiloxane) and used high-speed photography at 1 million frames per second to study the flow field. The PIV study demonstrated the 1/r dependency of the fluid velocity as function of the distance from the bubble center, and that the gross bubble dynamics can be modeled with a 2-dimensional Rayleigh model. The comparison is depicted in Fig. 1.

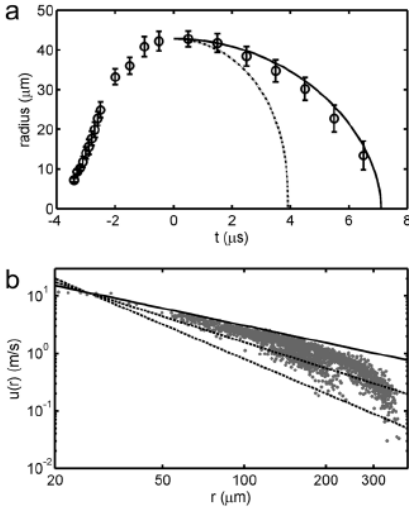


**Figure 1:** a) The measured bubble radius compared with a 2d (solid) and 3d-Rayleigh equation. b) Measured liquid velocity (gray points) as a function of the distance  $r$ . The top line has a slope of  $1/r$ . Picture has been adapted from Ref. 3.

At first sight it is rather surprising that a potential model neglecting viscosity is able to accurately describe the bubble dynamics in a narrow channel. Why are boundary layers not affecting the bubble dynamics? As we are focussing on the bubble shape in the centre of the channel there is a time associated for the growth of the boundary layers to the centre. It is the time needed for vorticity to diffuse from the boundaries which can be approximated with the time for the displacement thickness to reach to the channel's center

$$\tau = y^2 / (1.72^2 \nu), \quad (1)$$

where  $\nu$  is the viscosity and  $y$  is half the height of the liquid gap [4]. Thus, for these very brief times,  $t < \tau$ , the flow in the channels center is not affected by the no-slip boundary conditions as it is decoupled from the boundary layers; this allows to decompose the flow in a flow at the channel's center and a flow at the boundaries. The latter is a viscosity dominated boundary layer flow whereas the central flow is basically irrotational. Thus the flow in the center of the channel can be modeled for sufficiently short times with a velocity potential  $\Phi = \Phi(\mathbf{r}, t < \tau)$  which satisfies the Laplace equation:

$$\nabla^2 \phi = 0. \quad (2)$$

Assuming the viscosity of water,  $\nu = 10^{-6} \text{ m}^2 \text{ s}^{-2}$ , and a half-channel height of  $10 \mu\text{m}$  we obtain a "potential life-time" of  $\tau \approx 33 \mu\text{s}$ . Thus, for times shorter this duration the bubble dynamics in the center of the channel is essentially experiencing an irrotational flow.

Viscosity cause normal stresses at the bubble wall, too; however, for low viscous fluids such as water they can be safely ignored when compared to the ambient pressure.

## THEORY

Quinto-Su and Ohl have developed a potential model for  $N$ -bubble interaction based on a Lagrangian description of cylindrical bubbles [5]. It consists of two sets of  $N$ -equations. One equation for the radial dynamics

$$(\ddot{R}_i R_i + \dot{R}_i^2) \log\left(\frac{R_i}{R_\infty}\right) + \frac{\dot{R}_i^2}{2} = \frac{p}{\rho} - \frac{\mathbf{U}_i^2}{2} - \sum_{k \neq i} (\ddot{R}_k R_k + \dot{R}_k^2) \log\left(\frac{r_{ik}}{R_\infty}\right) \quad (3)$$

and one for the translational dynamics

$$\mathbf{r}_{0i} \ddot{\mathbf{r}}_i = -\frac{2\dot{R}_i \mathbf{U}_i}{R_i} + \sum_{k \neq i} \frac{\mathbf{n}_{ki} (R_k \ddot{R}_k + \dot{R}_k^2)}{r_{ki}} \quad (4)$$

Here,  $R$ , is the radius of the bubble,  $\mathbf{r}_{0i}$  the position vector of bubble  $i$ ,  $\mathbf{U}_i$  the translational velocity,  $\mathbf{n}_{ki}$  the normal vector pointing from bubble  $k$  to bubble  $i$ , and  $r_{ki}$  the distance between these bubbles. The density of the liquid is  $\rho$  and  $p$  is the pressure at infinity. Equation (3) is a two-dimensional Rayleigh equation with additional terms: the second term on the RHS of Eq. (3) is a Bernoulli pressure due to the bubble motion, and the third term due to the induced pressure from neighbouring bubbles. The quantity  $R_\infty$  is the distance at which the radial velocity drops to zero and can be identified with the distance to channel walls. Equation (4) can be read as a force balance with the first term on the right side being the added mass of the liquid due to the bubble motion and the second term a secondary *Bjerknes* force.

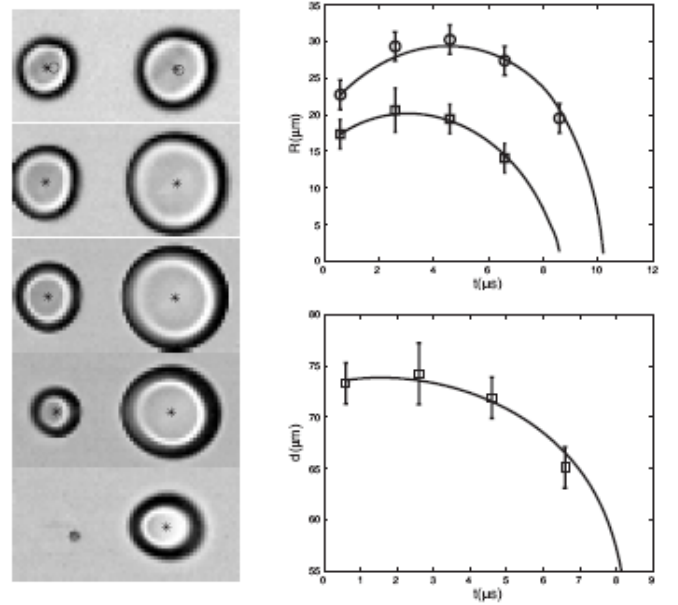


**Figure 2:** Left: Two bubbles created at a distance of  $70 \mu\text{m}$ . The framing speed is  $500,000 \text{ fps}$  and the frame width is  $128 \mu\text{m}$ . The last frame depicts on the left the remains from smaller bubble after its first collapse. Right top: Symbols showing the measured radii as a function of time for each bubble. Right bottom: Distance between the bubbles centers as a function of time. The solid lines are solutions of the two-dimensional potential model, Eqs. (3) and (4).

Interestingly, the *Bjerknes* force drops here with the inverse of the distance, e.g.  $r^{-1}$ , as compared to the well know result in 3-dimensions where it drops with  $r^{-2}$ . Thus the interaction between bubbles is longer ranged in 2-dimensions.

## COMPARISON WITH EXPERIMENTS

The model presented above has been tested with several two-bubble configurations and agrees convincingly with the observed dynamics. We present exemplarily in the left of Fig. 2 a photographic series of two unequally sized bubbles photographed in a gap of  $15\mu\text{m}$  height and recorded with 500,000 frames/s. The left and smaller bubble collapses first and the larger bubble obtains in the last frame a pointed shape. The initial conditions for the translational and radial dynamics are needed to integrate the equations of motion, Eqs. (3) and (4), because we ignore the early stage of the bubble formation. The initial values for bubble radius and bubble position are obtained from the experimental data. The initial conditions for the bubble wall and the translational velocities are obtained by least-square fitting of Eqs. (3) and (4) to the experimental data. Also a unique value for  $R_c$  for our experimental configuration has to be obtained. Details are given in Ref. [5]. The model describes the observed dynamics for all bubble pairs studied, in particular for the pair presented in Fig. 2.

## ON-DEMAND FLOW PATTERN GENERATION

We have selected the example of an unequally sized bubble pair because of the interesting flow pattern generated by it. The reader may consider first a couple of equally sized bubbles with their centres  $2d$  apart. In potential flow this geometry is equivalent to one bubble a distance  $d$  away from a rigid boundary. We know this bubble will jet towards the wall, thus two equally sized bubbles will jet towards each other. However, if one of the bubble is smaller than the other, it will create a jet first. After the collapse the second and larger bubble does not “see” the smaller bubble the jetting from the larger bubble is less strong, i.e. when both flows are superimposed the jetting from the smaller bubble prevails and directed flow is generated.

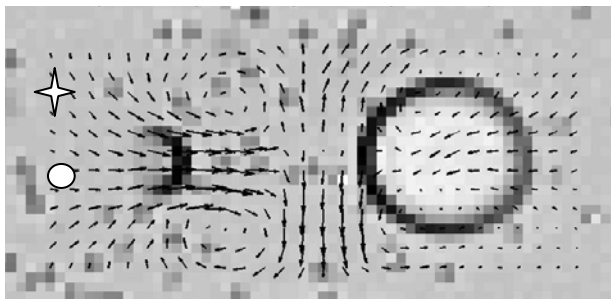


**Figure 3:** Averaged flow pattern generated from a bubble-couple shown in Fig. 2 left after both bubbles have collapsed. One picture showing the shape of the bubbles just before the collapse of the smaller bubble visualizes the geometry. The velocity vectors have been measured with particle image tracking velocimetry.

Figure 3 shows the averaged flow field induced by the bubble couple shown in Fig. 2 after the collapse both bubbles. The velocity vectors are overlaid on a picture demonstrating the jetting of the smaller bubble. This smaller bubble “wins” the jetting competition and creates a central stream from the left. At the centre the flow separates up or downward direction. Now consider an object located at the position indicated with a circle in Fig. 3. It will move towards the right, however, from the star position the object will move under an angle of 90 degree. This allows to direct and to manipulate objects in microfluidic environment by laser generated bubbles.

## NOVEL APPLICATIONS

**Transport of objects** can be achieved with the on-demand generated flow pattern as shown in Fig. 3.

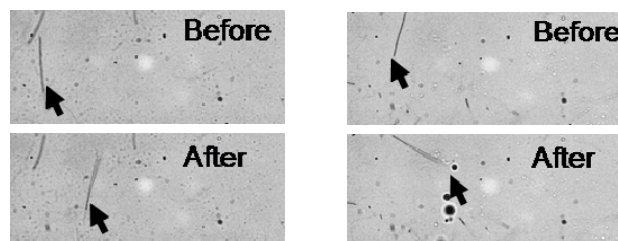


**Figure 4:** Left: Transport of a nanotube ( $30\mu\text{m}$  long and  $100\text{nm}$  thick) from left to right. Right: Anti-clockwise rotation of the nanotube

This is demonstrated here using a carbon nanotube as an object. The nanotube positioned with its center approximately at the circle in Fig. 3 translates towards the right as demonstrated in Fig. 4 right. When it is located initially a bit higher up, it will be exposed to the bending flow. Interestingly, the wire aligns with the flow, thus it rotates anti-clockwise. We explain this rotation by the strong direction dependent drag coefficient of the nanotube. This experiment demonstrates the transport of microscopic objects through cavitation induced flows. Possible application may be the assembling of nanowire/nanotube based electronic circuits and the measurement of elastic properties of these objects.

Next we summarize a few more applications of cavitation based microfluidics reported in literature:

**Mixing of liquids** at the interface of two co-flowing laminar flows was demonstrated by Hellman *et al.* [6]. A single bubble with a size comparable with the channel width and height creates vortices from liquid jets which quickly stir and mix both liquids.

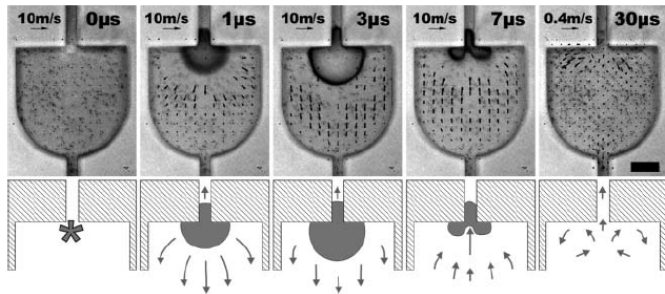


**Figure 5:** Selected high speed movie frames showing different stages of the bubble growth and collapse. The first image shows the chamber just before bubble initiation, then  $1\mu\text{s}$  later the bubble is rapidly expanding, reaching its maximum size in the third image ( $t = 3\mu\text{s}$ ). Afterwards the bubble starts to collapse creating a jet which is directed into the channel as can be seen in the fourth image. The black bar denotes  $50\mu\text{m}$ , picture adapted from Ref. 7.

A **bubble based pump** was demonstrated by Dijkink and Ohl [7]. Its pumping operation in the upward direction is shown in Figure 2. It is based on the fact that a bubble created close to a boundary jets towards it; with a hole in the boundary the bubble dynamics is hardly changed, yet the fluid is pushed through the hole.

The explosive growth of bubbles in an elastic channels can be used to actuate a **fluid switch** to push objects, e.g. cells, into a second channel [8]. Thereby rapid on demand sorting can be achieved.

In close-range interaction of cells with a cavitation bubble **creates pores** through which exterior molecules can be delivered into a cell's cytoplasm [9] or to cause rapid **cell lysis** [10].

Using a spatial light modular allows to generate **complex flow patterns**. Experimentally this is realized with a digital hologram altering the phase of the collimated beam which leads to a "Fourier" transformed intensity pattern in the focal plane of the focusing lens. This way very complex bubble patterns can be achieved as demonstrated in Fig. 3 and detailed more in Ref. 11.

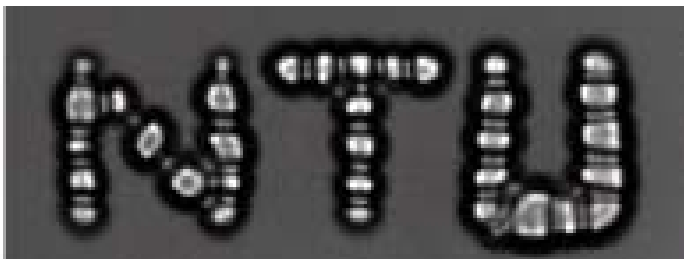


**Figure 6:** Bubble cluster consisting of 34 individual bubbles created with a computer controlled hologram.

As evident from Fig. 6, bubble can be strongly deformed. In this example the deformation is due to the bubble-bubble interaction. However, bubbles can be deliberately generated non-spherically by focusing the laser not on points/discs but on

more complex shapes. Programming the hologram with a circle focus gives rise to a donut shaped bubble as shown in Fig. 7.

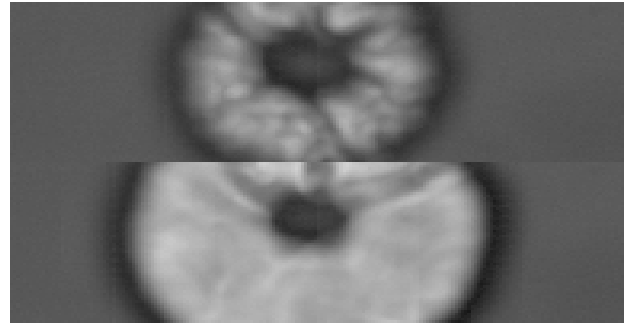


**Figure 7:** Toroidal bubble generated with an annular laser focus.

## SUMMARY

Cavitation bubbles in microfluidics may be described for sufficiently short times with a potential flow. The interaction of multiple bubbles allow the generation of complex flow patterns. These flow patterns can be used to transport microscopic objects and to rotate them. Several important fluid mechanic applications have been demonstrated in so far in literature, mixing, switching, pumping, and perforation of biological cells. Using the pulsed laser together with a digital hologram allows the generation of almost arbitrary flow patterns promising novel solutions in microfluidic applications.

## ACKNOWLEDGMENTS

We like to thank Lim Kang Yuan for his help with the experiments on non-spherical bubbles (Fig.7). Further we thank MOE and NTU, both Singapore for their financial contributions under grants T208A1238 and RG39/07, NWO, The Netherlands, and NIH U.S. under grants P41-RR01192 and R01-EB04436.

## REFERENCES

- [1] Chen, Y. L., Israelevachvili, J., 1991, "New Mechanism of Cavitation," *Science*, May 24, 252, 1157-1160.
- [2] Chen, Y. H., Chu, H. Y., I., L., 2006, "Interaction and fragmentation of pulsed laser induced microbubbles in a narrow gap," *Physical Review Letters*, 96, 034505.
- [3] Zwaan, E. Le Gac, S. Tsuji, K., Ohl, C. D., 2007, "Controlled cavitation in microfluidic systems" *Physical Review Letters*, 98, 254501.
- [4] Batchelor, G. K. 1967 *An Introduction to Fluid Dynamics*. Cambridge University Press.
- [5] Quito-Su, P.A., Ohl, C.D., 2009, "Interaction between two laser-induced cavitation bubbles in a quasi-two dimensional geometry", *J. Fluid Mech.* In press.
- [6] Hellman A. N., Rau K. R., Yoon H. H., Bae S., Palmer J. F., Phillips K. S., Allbritton N. L., Venugopalan V., 2007, "Laser-induced mixing in microfluidic channels," *Analytical Chemistry*, 79, 4484-4492.

- [7] Dijkink, R., Ohl, C. D., “Laser-induced cavitation based micropump”, *Lab On A Chip*, 8, 1676-1681.
- [8] Wu, T. H., Gao, L. Y., Chen, Y., Wei K., Chiou P. Y., 2008, “Pulsed laser triggered high speed microfluidic switch,” *Applied Physics Letters*, 93 144102.
- [9] Le Gac, S., Zwaan, E., van den Berg, A., Ohl, C.D., 2007, “Sonoporation of suspension cells with a single cavitation bubble in a microfluidic confinement,” *Lab On A Chip*, 7, 1666-1672.
- [10] Quinto-Su P. A., Lai H. H., Yoon H. H., Sims C. E., Allbritton N. L., Venugopalan V. , 2008, “Examination of laser microbeam cell lysis in a PDMS microfluidic channel using time-resolved imaging,” *Lab On A Chip*, 8, 408-414.
- [11] Quinto-Su, P. A., Venugopalan, V., Ohl, C.D., 2008, “Generation of laser-induced cavitation bubbles with a digital hologram”, *Optics Express*, 16 18964-18969.